Time-Resolved Resonance Raman Study of Triplet Arylnitrenes and Their Dimerization Reaction

Shing Yau Ong, Pik Ying Chan, Peizhi Zhu, King Hung Leung, and David Lee Phillips*

Department of Chemistry, The University of Hong Kong, Pokfulam Road, Hong Kong S. A. R., P. R. China

Received: June 21, 2002; In Final Form: November 6, 2002

Time-resolved resonance Raman spectra for triplet 4-methoxyphenyl nitrene and 4-ethoxyphenyl nitrene and their dimerization reaction to form azo dimer products in acetonitrile solution on the nanosecond time scale are reported. As the 4-methoxyphenyl nitrene and 4-ethoxyphenyl nitrene Raman bands decay, the Raman bands for the azo dimer products increase in intensity. The triplet 4-methoxyphenyl nitrene and 4-ethoxyphenyl nitrene species and their reaction to produce azo products are compared to a recent study of the 2-fluorenyl nitrene species and its reaction to form dehydroazepine ring-expansion products. The properties of the singlet and triplet arylnitrenes and their reaction mechanisms to form azo dimer and ring-expansion products are briefly discussed.

Introduction

The photochemistry of aryl azides[1−53] has been an important and active area of research. The use of laser flash photolysis techniques over the past decade to probe their reaction intermediates and photoproducts directly has led to an improved understanding of their reaction mechanisms and intermediates. Ultraviolet excitation of aryl azides in solutions usually produces a singlet nitrene species that may then either undergo a very rapid ring expansion to produce ketenimines (dehydroazepine) or decay via rapid intersystem crossing to the triplet nitrene species that may then subsequently produce azo dimerization products. The singlet arylnitrene ring-expansion products, ketenimines (dehydroazepines), can be trapped by nucleophiles. The singlet phenyl nitrene chemistry and reaction mechanisms have been particularly well examined and characterized.[7,8,18,20,21,40−44,48−50] Laser flash photolysis experiments have been used to observe singlet phenyl nitrene directly in room-temperature solutions.[42,43] The singlet phenyl nitrene species has a short lifetime of about 1 ns because of its fast ring-expansion reaction,[42,43] but the lifetimes of other singlet nitrenes can become substantially longer when various substituents are used.[16−18,22−25,28,39,51,53] For example, singlet nitrenes with lifetimes of tens to hundreds of nanoseconds[39] can be made from the photolysis of polyfluorinated phenyl azides in acetonitrile solutions because the ring-expansion reaction becomes slower because of a higher activation barrier.[16−18,22−25,28,39,51,53] Nucleophiles such as diethylamine, pyridine, and tetramethylethylene have been used to trap some of these longer-lived singlet nitrene species chemically. Singlet arylnitrenes have also been found to react readily with water to produce singlet nitrenium ions.[26,27,30−36,39,45,46,54,55] However, there are few studies of direct vibrational spectroscopic characterization of arylnitrenes in room-temperature solutions.[56]

In this paper, we present a time-resolved resonance Raman spectroscopic study of triplet arylnitrenes produced following ultraviolet photolysis of 4-methoxyphenyl azide and 4-ethoxyphenyl azide in acetonitrile solutions. To our knowledge, these are the first time-resolved resonance Raman spectra obtained for triplet arylnitrenes and their reaction to form azo products in room-temperature solutions. As the time delay between the pump (266 nm) and probe (320 nm) pulses change from 10 to 500 ns, some Raman bands decay in intensity, and others increase in intensity, indicating that there are two species present and that the first species decays to form the second species. The Raman vibrational frequencies for the first species exhibit good agreement with those calculated from density functional theory for triplet 4-methoxyphenyl nitrene and 4-ethoxyphenylnitrene, and the second species vibrational frequencies show reasonable agreement with the computed frequencies for the azo product formed from the triplet nitrenes. In addition, the resonance Raman spectrum of an authentic sample of the 4-methoxyphenylnitrene azo dimer product produced from another synthetic method was essentially identical to the time-resolved resonance Raman spectrum of the second photoproduct species observed after the photolysis of 4-methoxy phenyl azide. This confirms the assignment of the second photoproduct species in the time-resolved resonance Raman experiments to the azo dimer product. We compare the triplet 4-methoxyphenyl nitrene and 4-ethoxyphenyl nitrene species and their reaction to produce azo products to a recent study of the singlet 2-fluorenyl nitrene species and its reaction to form dehydroazepine products.[56] We briefly discuss the properties of the singlet and triplet arylnitrenes and their reaction mechanisms.

Experimental and Calculations Section

Samples of 4-methoxyphenyl azide and 4-ethoxyphenyl azide were synthesized according to literature methods,[57] and further details of the synthesis and characterization are given in the Supporting Information. The 4-methoxyphenyl azide and 4-ethoxyphenyl azide samples were prepared with concentrations in the 2.3−2.4 mM range in acetonitrile solvent for the time-resolved resonance Raman experiments. An authentic sample of the 4-methoxyphenylnitrene azo dimer product (4,4′-dimethoxyazobenzene) was synthesized by following a literature procedure,[58] and further details of the synthesis and character-

* Author to whom correspondence should be addressed. E-mail: phillips@hkucc.hku.hk.

10.1021/jp021468m CCC: $25.00
Published on Web 04/19/2003

ization are presented in the Supporting Information. The 4,4′-dimethoxyazobenzene sample was prepared with a 1.2 mM concentration in acetonitrile solvent for the single-beam 320-nm resonance Raman experiment.

The time-resolved resonance Raman instrument and methods have been described elsewhere, and only a short description is given here.[56,59,60] The time-resolved resonance Raman experiments used two Nd:YAG lasers (Spectra-Physics) that were electronically synchronized to one another via a pulse-delay generator (Stanford Research Systems model DG535) used to control the relative timing of the lamp and Q-switch firing of the two lasers. A fast photodiode whose output was shown on a 500-MHz oscilloscope was used to measure the relative timing of the pump (266 nm) and probe (320 nm) laser pulses. The laser beams were loosely focused onto a flowing liquid stream of sample using a near-collinear geometry, and the Raman scattered light was collected using reflective optics. A back-scattering geometry was used to acquire the Raman scattered light, and it was imaged through a polarization scrambler mounted on the entrance slit of a 0.5-m spectrograph. The spectrograph grating dispersed the Raman light onto a liquid nitrogen-cooled CCD detector that acquired the Raman signal for ∼300 to 600 s before being read out to an interfaced PC. About 10 to 20 of the readouts were summed to get a resonance Raman spectrum. Pump-only, probe-only, and pump−probe resonance Raman spectra were taken in addition to a background scan. The known Raman bands of the acetonitrile solvent were used to calibrate the Raman wavenumber shifts of the spectra. The probe-only spectrum was subtracted from the pump−probe spectrum to remove solvent and precursor Raman bands so as to obtain the time-resolved Raman spectrum. (In addition, the pump-only spectrum and the background spectrum were also subtracted from the pump−probe spectrum.)

All of the density functional calculations employed the Gaussian program suite.[61] Complete geometry optimization and vibrational frequency calculations were made analytically with the UBPW91 or BPW91 method[62,63] and the cc-PVDZ basis set[64] for the singlet and triplet states of the 4-methoxyphenyl nitrene and 4-ethoxyphenyl nitrene species as well as for their possible azo and dehydroazepine products.

Results and Discussion

Figures 1 and 2 present an overview of the 320-nm probe time-resolved resonance Raman spectra obtained for the photoproducts generated over the 10- to 500-ns time scale following 266-nm photolysis of 4-methoxyphenyl azide and 4-ethoxyphenyl azide, respectively, in acetonitrile solutions. Figures 3 and 4 present an expanded view of the 10- and 500-ns time-resolved spectra shown in Figures 1 and 2, respectively. An inspection of Figures 1 and 2 reveals that some Raman bands decrease in intensity over the 10- to 500-ns time scale while other Raman bands increase in intensity. This indicates the presence of two photoproduct species with the first species likely decaying into the second product. The 10-ns spectra shown in Figures 3 and 4 show Raman bands from both photoproduct species whereas the 500-ns spectra exhibit mainly Raman bands from the second species. Figure 5 displays a plot of the time-dependent behavior of the five largest resonance Raman bands of the first and second photoproduct species observed after the photolysis of 4-methoxyphenyl azide in acetonitrile solvent. Simple exponential decay/growth best-fit curves for the plots are shown as lines in Figure 5. An inspection of Figure 5 shows that the decay rates of the five Raman bands of the first photoproduct species are

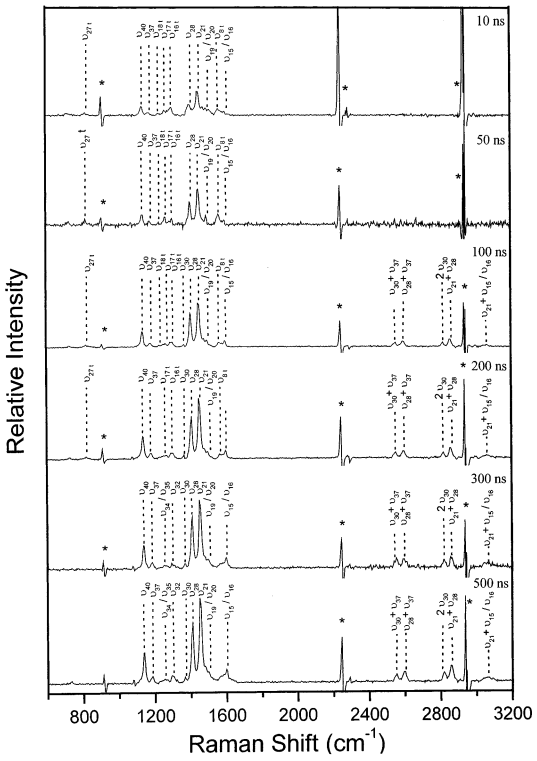

Figure 1. Time-resolved resonance Raman spectra acquired after 266-nm photolysis of 4-methoxyphenyl azide in acetonitrile using a 320-nm probe wavelength. The time-resolved resonance Raman spectra were obtained by subtracting probe-only spectra and pump-only spectra from pump/probe spectra to remove solvent and azide precursor Raman bands. The spectra were acquired with different pump/probe time delays (10, 50, 100, 200, 300, and 500 ns), as indicated next to each spectrum. Asterisks mark solvent-subtraction artifacts. Tentative vibrational assignments for some of the Raman bands are labeled. (Refer to the text and Table 1 for more details.) Raman band assignments with a "t" represent triplet 4-methoxyphenyl nitrene features, and the others are due to its azo dimer product.

almost the same, and this is consistent with these Raman bands belonging to the same photoproduct species. Similarly, the five largest Raman bands of the increasing photoproduct(s) increase at almost the same rate, and this is consistent with these Raman bands belonging to the same photoproduct species. The first photoproduct species decays approximately twice as fast as the second species grows, and this is consistent with a reaction of the first species with itself to produce a dimer species product (e.g., species 1 + species 1 → species 2). Very similar behavior was also observed for the time-resolved resonance Raman spectra observed after the photolysis of 4-ethoxyphenyl azide in acetonitrile solvent.

Several investigations have used a comparison of experimental vibrational frequencies to those predicted from density functional theory or ab initio calculations for probable photoproduct species to assign time-resolved infrared or Raman spectra to arylnitrenium ions, arylnitrenes, and arylnitrene photoproducts.[46,52,54−56] We shall use a similar approach here to help in the assignment of the spectra observed in Figures 1−4. We have made UBPW91/cc-PVDZ computations for the singlet and triplet states of the 4-methoxyphenyl nitrene and 4-ethoxyphenyl nitrene species and BPW91/cc-PVDZ calculations for their potential azo products (denoted hereafter as A-OMe and A-OEt, respectively) and their dehydroazepine products (denoted as DH-OMe and DH-OEt, respectively). Tables 1 and 2 compare the experimental Raman vibrational frequencies to those predicted from the density functional theory calculations for the

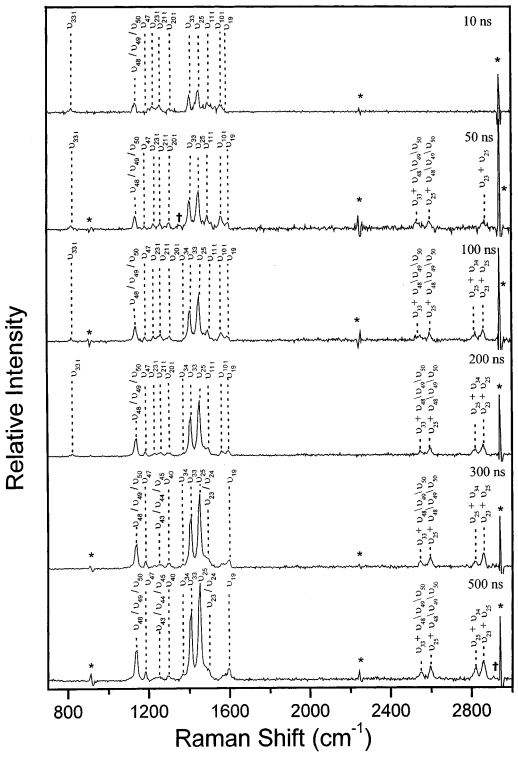

Figure 2. Time-resolved resonance Raman spectra acquired after 266-nm photolysis of 4-ethoxyphenyl azide in acetonitrile using a 320-nm probe wavelength. The time-resolved resonance Raman spectra were obtained by subtracting probe-only spectra and pump-only spectra from pump/probe spectra to remove solvent and azide precursor Raman bands. The spectra were acquired with different pump/probe time delays (10, 50, 100, 200, 300, and 500 ns), as indicated next to each spectrum. Asterisks mark solvent-subtraction artifacts, and daggers represent small stray-light or ambient-light artifacts. Tentative vibrational assignments for some of the Raman bands are labeled. (Refer to the text and Table 2 for more details.) Raman band assignments with a "t" represent triplet 4-ethoxyphenyl nitrene features, and the others are due to its azo dimer product.

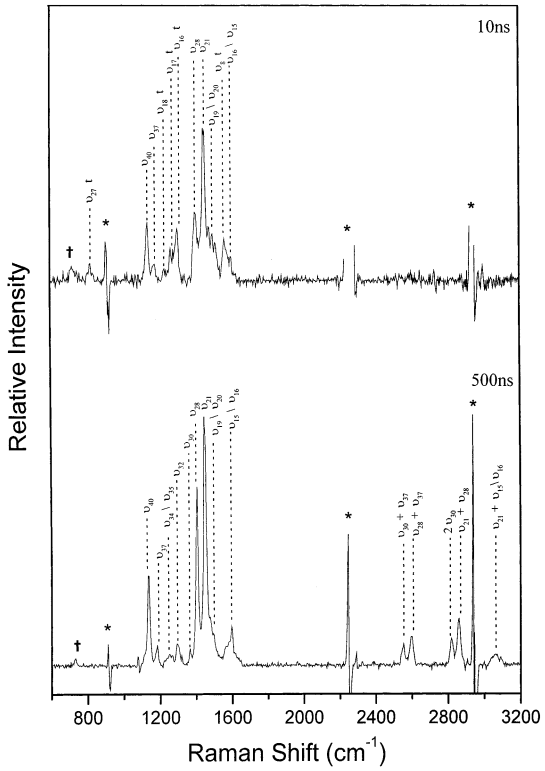

Figure 3. Expanded view of the 10- and 500-ns time-resolved resonance Raman spectra shown in Figure 1. Asterisks mark solvent-subtraction artifacts, and daggers represent small stray-light or ambient-light artifacts. Tentative vibrational assignments for the larger Raman bands are labeled. (Refer to the text and Table 1 for more details.) Raman band assignments with a "t" represent triplet 4-methoxyphenyl nitrene features, and the others are due to its azo dimer product.

4-methoxyphenyl nitrene and 4-ethoxyphenyl nitrene species and their azo and dehydroazepine products, respectively.

An inspection of Table 1 shows that the short-lived Raman band species formed after the photolysis of 4-methoxyphenyl azide are in better agreement with those of the triplet 4-methoxyphenyl nitrene species than with those of the singlet state. The triplet state shows a difference on average of about 6.4 cm^{-1} between the experimental and computed vibrational frequencies compared to 11.8 cm^{-1} for the singlet state. Similarly, Table 2 also shows that the short-lived species Raman band vibrational frequencies formed after the photolysis of 4-ethoxyphenyl azide are in better agreement with those of the triplet 4-ethoxyphenyl nitrene species than with those of the singlet state. The triplet state exhibits a difference on average of about 8 cm^{-1} between the experimental and computed vibrational frequencies compared to 12.3 cm^{-1} for the singlet state. Thus, it is tempting to assign the first species to the triplet states of 4-methoxyphenyl nitrene and 4-ethoxyphenyl nitrene, respectively. However, the calculations are probably not good enough to distinguish clearly between the triplet and singlet nitrenes since both are within the $\sim$10$-$20 cm^{-1} error of margin of the calculations, and further evidence is needed to assign the first product species clearly. The $\langle s^2 \rangle$ values from the calculations are given in Supporting Information for the singlet and triplet nitrene species examined here. These $\langle s^2 \rangle$ values indicate that there is some moderate spin contamination in the open-shell singlet nitrene from the triplet state. Thus, the singlet nitrene computational results are probably not accurate enough to make an unambiguous comparison to the experimental vibrational data. However, the $\langle s^2 \rangle$ values indicate that there is no appreciable spin contamination of the triplet-state calculations, and these can be used for comparison with the experimental vibrational spectra. Our comparison of the experimental and computed results indicates that the vibrational frequencies observed for the first product species are consistent with those computed for the triplet arylnitrene species, but we cannot exclude the singlet arylnitrene species on the basis of the computational results.

An examination of Table 1 shows that the second longer-lived species formed after the photolysis of 4-methoxyphenyl azide has Raman band vibrational frequencies that are in better agreement with those of the dimer product (A-OMe) formed from the 4-methoxyphenyl nitrene species than with those of the dehydroazepine ring-expansion product (DH-OMe). The azo product (A-OMe) shows a difference on average of about 7 cm^{-1} between the experimental and computed vibrational frequencies compared to 15.8 cm^{-1} for the dehydroazepine ring-expansion product (DH-OMe). Similarly, Table 2 indicates that the Raman vibrational frequencies of the second longer-lived Raman band species formed after the photolysis of 4-ethoxyphenyl azide are in better agreement with those of the azo product (A-OEt) formed from the triplet 4-ethoxyphenyl nitrene species than with those of the dehydroazepine ring-expansion product (DH-OEt). The azo product (A-OEt) exhibits a difference on average of about 7.4 to 8.4 cm^{-1} between the experimental and computed vibrational frequencies compared to 13 cm^{-1} for the dehydroazepine ring-expansion product (DH-OEt). Therefore, we assign the second species to azo

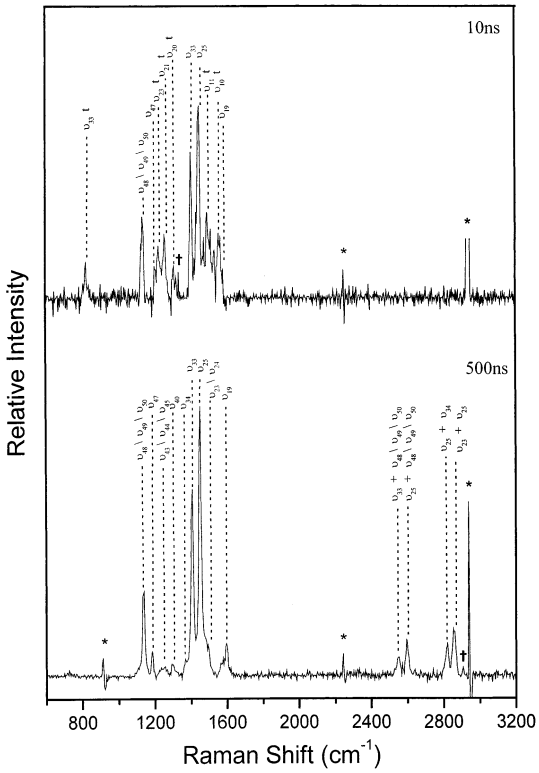

Figure 4. Expanded view of the 10- and 500-ns time-resolved resonance Raman spectra shown in Figure 2. Asterisks mark solvent-subtraction artifacts, and daggers represent small stray-light or ambient-light artifacts. Tentative vibrational assignments for the larger Raman bands are labeled. (Refer to text and Table 2 for more details.) Raman band assignments with a "t" represent triplet 4-ethoxyphenyl nitrene features, and the others are due to its azo dimer product.

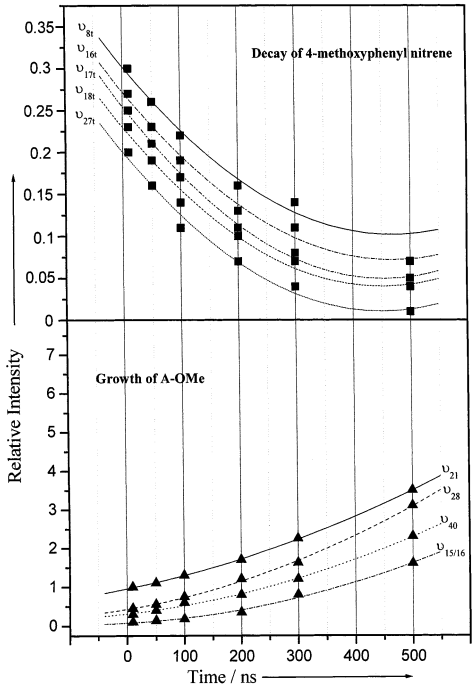

Figure 5. Plot of the time-dependent behavior of the five largest resonance Raman bands of the first (scale on left and decaying species) and second (scale on right and growing species) photoproduct species observed in Figure 1 after the photolysis of 4-methoxyphenyl azide in acetonitrile solvent. Simple exponential decay/growth best-fit curves for the plots are shown as lines.

products A-OMe and A-OEt of the triplet 4-methoxyphenyl nitrene and 4-ethoxyphenyl nitrene, respectively. The resonance Raman intensity pattern of the second species observed in the time-resolved resonance Raman spectra of Figures 1−4 is similar to that of resonance Raman spectra observed for a number of azo compounds with phenyl groups (such as *trans*-azobenzene, 4-nitro,4′-dimethyolamino-azo benzene, and others)[65−72] that have most of their intensity in the 1400−1500 cm^{-1} region for modes associated with the N═N chromophore and significant intensity in their overtones and/or combination bands in the 2800−3000 cm^{-1} region. This provides additional support for our assignment of the second species to azo products A-OMe and A-OEt of the triplet 4-methoxyphenyl and 4-ethoxyphenyl nitrenes, respectively. To determine the identity of the second photoproduct species observed in the TR^3 spectra in Figures 1−4 unambiguously, we synthesized an authentic sample of the azo dimer product formed from 4-methoxyphenylnitrene (4,4′-dimethoxyazobenzene). The 4,4′-dimethoxyazobenzene sample was made by oxidizing the appropriate aniline as described in ref 58 and in the Supporting Information. We obtained a 320-nm resonance Raman spectrum of this authentic 4,4′-dimethoxyazobenzene sample. Figure 6 compares the authentic 4,4′-dimethoxyazobenzene sample's 320-nm resonance Raman spectrum to the TR^3 spectrum obtained at 500 ns following 266-nm photolysis of 4-methoxyphenyl azide using a 320-nm probe wavelength. A comparison of the spectra in Figure 6 shows that they are almost identical in both vibrational frequencies and intensities. This conclusively demonstrates that the second photoproduct species observed in the TR^3 spectra is due to the azo dimer photoproduct and not to a dehydroazepine product.

The clear assignment of the second photoproduct species observed in the TR^3 spectra to the azo dimer product and the observation that the first photoproduct species decays approximately twice as fast as the second species grows indicate that the reaction of the first species with itself produces the azo dimer product. Singlet arylnitrenes such as phenylnitrene tend to react and form ring-expansion dehydroazepine products whereas triplet nitrenes such as phenylnitrene tend to form azo dimerization products with a N═N group in the condensed phase.[3−9] This indicates that the first photoproduct species observed in the TR^3 spectra of Figures 1−4 should be assigned to the triplet 4-methoxyphenyl nitrene and triplet 4-ethoxyphenyl nitrene species.

We note that our assignments of the two species observed in the time-resolved resonance Raman spectra of Figures 1−4 are consistent with a number of previous experimental studies of para-substituted phenyl nitrenes.[15,50] An earlier study using time-resolved ultraviolet absorption and infrared spectroscopy found that the photolysis of 4-methoxyphenyl azide in cyclohexane produced an 80% yield of the dimer product from triplet nitrene (A-OMe) whereas photolysis in the presence of diethylamine gave a 27% yield of the ketenimine adduct.[15] These results indicate that both triplet nitrene (formed from the singlet nitrene and associated with the azo product) and dehydroazepine products (formed from the singlet nitrene and associated with the ketenimine adduct) are formed to some extent in room-temperature solutions.[15] More recent studies using laser flash photolysis and product analysis found that the photolysis of 4-methoxyphenyl azide in pentane solution produced a transient absorption spectrum of its triplet nitrene and the ketenimine products over a 100-ns window just after the photolysis pulse and that the intersystem crossing (ISC) from the initially produced singlet nitrene decayed very quickly to the triplet state (with a rate constant estimated to be $>500 \times 10^6$ s^{-1} and $\tau <$ 1 ns).[50] The triplet nitrene exhibits a strong absorption with λ_{max}

TABLE 1: Experimental Raman Vibrational Frequencies Observed in the Time-Resolved Resonance Raman Spectra of 4-Methoxyphenyl Nitrene and Its Azo Product Shown in Figures 1 and 3[a]

A. 4-Methoxyphenyl Nitrene Species Observed in the 10-,50-, and 100-ns Time-Resolved Resonance Raman Spectra

singlet 4-methoxyphenyl nitrene		tripet 4-methoxyphenyl nitrene		experiment
vibrational mode, possible description	UBPW91/cc-PVDZ calcd value (in cm^{-1})	vibrational mode, possible description	UBPW91/cc-PVDZ calcd value (in cm^{-1})	10-ns time-resolved Raman freq shift (cm^{-1})
ν_{29}, C−H bend	758	ν_{29}, C−H bend		768
ν_{28}, C−H bend	808	ν_{28}, C−H bend		810
ν_{27}, CCC bend	810	**ν_{27}, CCC bend**	**824**	**824**
ν_{26}, C−H bend	911	ν_{26}, C−H bend		914
ν_{25}, C−H bend	937	ν_{25}, C−H bend		938
ν_{24}, CCC bend	951	ν_{24}, CCC bend		958
ν_{23}, CCC bend + C−O str	1025	ν_{23}, CCC bend + C−O str		1027
ν_{22}, C−C str + C−H bend	1077	ν_{22}, C−C str + C−H bend		1081
ν_{21}, CH_3 bend	1116	ν_{21}, CH_3 bend		1117
ν_{20}, C−H bend	1133	ν_{20}, C−H bend		1131
ν_{19}, C−H bend + CH_3 bend	1155	ν_{19}, CH_3 bend	1156	
ν_{18}, C−C str	1222	**ν_{18}, C−C str**	**1235**	**1232**
ν_{17}, C−C str + C−O str	1257	**ν_{17}, C−C str + C−O str**	**1256**	**1265**
ν_{16}, C−C str + C−O str	1283	**ν_{16}, C−C str + C−O str**	**1291**	**1301**
ν_{15}, C−C str + C−N str	1379	ν_{15}, C−C str + C−N str		1322
ν_{14}, C−C str + C−N str	1412	ν_{14}, CH_3 bend + C−N str		1403
ν_{13}, CH_3 bend	1420	ν_{13}, CH_3 bend		1420
ν_{12}, C−C str + C−N str	1424	ν_{12}, C−C str + CH_3 bend		1422
ν_{11}, C−C str + CH_3 bend	1432	ν_{11}, C−C str + CH_3 bend		1433
ν_{10}, C−C str+CH_3 bend + C−N str	1446	ν_{10}, C−C str + C−N str + C−O str		1445
ν_9, C−C str	1485	ν_9, C−C str		1499
ν_8, C−O str + C−C str + C−N str	1584	**ν_8, C−N str + C−C str + C−O str**	**1585**	**1575**

B. Potential Dehydroazepine and Azo Product Species Observed in the 300- and 500-ns Time-Resolved Resonance Raman Spectra in Figures 1 and 2

dehydroazepine product (DH−OMe)		azo product (A-OMe)		experiment
vibrational mode, approximate description	BPW91/cc-PVDZ calcd value (cm^{-1})	vibrational mode, approximate description	BPW91/cc-PVDZ calcd value (in cm^{-1})	500-ns and 10-μs time-resolved Raman freq shift (cm^{-1})
ν_{21}, C−N=C str + C−H bend	1102	ν_{43}, CH_3 bend	1118	
ν_{20}, CH_3 bend	1118	ν_{42}, C−H bend	1118	
		ν_{41}, CH_3 bend	1120	
		ν_{40}, C−H bend + C−N str	**1121**	**1135**
ν_{19}, C−O str + C−H bend + CH_3 bend	1150	ν_{39}, CH_3 bend	1157	
		ν_{38}, CH_3 bend	1157	
ν_{18}, C−H bend + CH_3 bend	1178	**ν_{37}, C−C str + C−N str**	**1184**	**1184**
ν_{17}, C−C str + C−O str + C−H bend	1210	ν_{36}, C−C str + C−N str + C−O str	1229	
		ν_{35}, C−C str + C−N str + C−O str	**1254?**	**1254**
		ν_{34}, C−C str	**1256?**	
		ν_{33}, C−C str + C−N str + C−O str	1260	
ν_{16}, C−H bend	1268	**ν_{32}, C−C str + C−N str + C−O str**	**1265**	**1291**
ν_{15}, C−C str	1300	ν_{31}, C−C str	1358	
ν_{14}, C−H bend	1371	**ν_{30}, C−C str + N=N str**	**1366**	**1364**
		ν_{29}, CH_3 bend	1410	
ν_{13}, CH_3 bend	1410	**ν_{28}, C−C str + N=N str**	**1411**	**1408**
		ν_{27}, C−C str	1412	
ν_{12}, CH_3 bend	1417	ν_{26}, CH_3 bend	1418	
		ν_{25}, CH_3 bend	1420	
		ν_{24}, C−C str	1425	
ν_{11}, CH_3 bend	1433	ν_{23}, CH_3 bend + N=N str	1431	
		ν_{22}, C−C str	1436	
		ν_{21}, C−C str + N=N str	**1449**	**1448**
		ν_{20}, C−C str + N=N str + C−O str	**1486?**	
		ν_{19}, C−C str + N=N str + C−O str	**1489?**	**1495**
ν_{10}, C−C str	1543	ν_{18}, C−C str	1571	
ν_9, C−C str	1579	ν_{17}, C−C str	1574	
		ν_{16}, C−C str	**1611?**	
		ν_{15}, C−C str + C−O str + N=N str	**1616?**	**1603**

[a] Experimental vibrational frequencies are compared to those from UBPW91/cc-PVDZ computations for the singlet and triplet states of 4-methoxyphenyl nitrene (A) and those from BPW91/cc-PVDZ computations for the potential 4-methoxyphenyl nitrene dehydroazepine and azo products (B). See text for more details. Possible vibrational band assignments are also shown on the basis of comparisons to calculated vibrational frequencies from UBPW91/cc-PVDZ or BPW91/cc-PVDZ computations in the 750- to 1700-cm^{-1} fingerprint region for the ground singlet and triplet states of 4-methoxyphenyl nitrene and the ground singlet state of its dehydroazepine or azo products (see text).

≈ 330 nm. These results are in excellent agreement with our time-resolved resonance Raman spectra obtained using a 320-nm probe wavelength and with our observation of the triplet nitrene at delay times in the 10- to 200 ns region.

Triplet 4-methoxphenyl nitrene and 4-ethoxyphenyl nitrene decay and immediately form the azo dimer product in the time-resolved resonance Raman spectra shown in Figures 1 and 2 using a 320-nm probe wavelength. This behavior is in stark contrast to the time-resolved resonance Raman observation of the decay of the 2-fluorenyl nitrene species and the subsequent formation of its dehydroazepine ring-expansion product(s).[56] The 2-fluorenyl nitrene species decays within 100 to 500 ns to form

TABLE 2: Experimental Raman Vibrational Frequencies Observed in the Time-Resolved Resonance Raman Spectra of 4-Ethoxyphenyl Nitrene and Its Azo Product Shown in Figures 2 and 4[a]

A. 4-Ethoxyphenyl Nitrene Species Observed in the 10-, 50-, and 100-ns Time-Resolved Resonance Raman Spectra in Figures 3 and 4

singlet 4-ethoxyphemyl nitrene		tripet 4-ethoxyphenyl nitrene		experiment
vibrational mode, possible description	UBPW91/cc-PVDZ calcd value (cm^{-1})	vibrational mode, possible description	UBPW91/cc-PVDZ calcd value (cm^{-1})	10-ns time-resolved Raman freq shift (cm^{-1})
ν_{36}, C−H bend	756	ν_{36}, C−H bend	766	
ν_{35}, C−H bend	804	ν_{35}, ring def + CH_2 rock + CH_3 bend	805	
ν_{34}, C−H bend	811	ν_{34}, ring def + CH_2 rock + CH_3 bend	813	
ν_{33}, CCC bend	812	**ν_{33}, CCC bend**	**825**	**823**
ν_{32}, CCC bend	903	ν_{32}, CCC bend	907	
ν_{31}, C−H bend	910	ν_{31}, C−H bend	913	
ν_{30}, C−H bend	936	ν_{30}, C−H bend	937	
ν_{29}, C−H bend	954	ν_{29}, ring def	961	
ν_{28}, C−O str + C−C str	1029	ν_{28}, C−O str + C−C str	1035	
ν_{27}, C−C str + C−H bend	1077	ν_{27}, C−C str + C−H bend	1081	
ν_{26}, C−O str + C−C str	1093	ν_{26}, C−O str + C−C str	1099	
ν_{25}, CH_2 rock + CH_3 bend	1126	ν_{25}, CH_2 twist + CH_3 bend	1126	
ν_{24}, C−H bend	1132	ν_{24}, C−H bend	1130	
ν_{23}, C−C str + CH_2 wag	1221	**ν_{23}, C−C str**	**1235**	**1231**
ν_{22}, C−C str + C−O str	1248	ν_{22}, CH_2 twist + CH_3 bend	1250	
ν_{21}, CH_2 twist + CH_3 bend	1250	**ν_{21}, C−C str + C−O str**	**1253**	**1261**
ν_{20}, C−C str + C−O str	1287	**ν_{20}, C−C str + C−O str**	**1290**	**1306**
ν_{19}, CH_2 wag + C−H bend + CH_3 bend	1332	ν_{19}, C−N str + C−C str	1322	
ν_{18}, CH_2 wag + C−H bend + CH_3 bend	1366	ν_{18}, CH_2 wag + C−C str + C−N str	1339	
ν_{17}, C−C str + C−N str	1390	ν_{17}, CH_2 wag + C−C str	1368	
ν_{16}, CH_3 bend	1416	ν_{16}, CH_3 bend	1416	
ν_{15}, C−C str + C−N str + CH_2 sciss.	1422	ν_{15}, C−C str + C−N str	1421	
ν_{14}, C−C str + C−N str + CH_2 sciss	1433	ν_{14}, C−C str + CH_2 sciss + CH_3 bend	1432	
ν_{13}, C−C str + CH_3 bend	1437	ν_{13}, C−C str + CH_3 bend	1437	
ν_{12}, C−C str + CH_3 bend + CH_2 sciss	1456	ν_{12}, C−C str + CH_2 sciss	1454	
ν_{11}, C−C str	1484	**ν_{11}, C−C str**	**1497**	**1495**
ν_{10}, C−C str + C−O str	1584	**ν_{10}, C−C str + C−O str**	**1585**	**1572**

B. Potential Dehydroazepine and Azo Product Species Observed in the 300-and 500-ns Time-Resolved Resonance Raman Spectra in Figures 3 and 4

DH-OEe dehydroazepine product		A-OEe azo product		experiment
vibrational mode, approximate description	BPW91/cc-PVDZ calcd value (cm^{-1})	vibrational mode, approximate description	BPW91/cc-PVDZ calcd value (cm^{-1})	500-ns and 10-μs time-resolved Raman freq shift (cm^{-1})
ν_{25}, C−O str + C−C str + C−N str	1101	ν_{52}, C−O str + C−C str	1100	
		ν_{51}, C−H bend	1119	
		ν_{50}, C−N str + C−H bend	**1121?**	
ν_{24}, CH_2 rock + CH_3 bend	1124	**ν_{49}, CH_2 rock + CH_3 bend**	**1127?**	**1139**
		ν_{48}, CH_2 rock + CH_3 bend	**1127?**	
ν_{23}, C−O str + C−H bend	1174	**ν_{47}, C−C str + C−N str + C−O str**	**1184**	**1184**
ν_{22}, C−O str + C−C str + C−H bend	1214	ν_{46}, C−C str + C−N str + C−O str	1227	
		ν_{45}, CH_2 twist + CH_3 bend	**1246?**	
		ν_{44}, CH_2 twist + CH_3 bend	**1246?**	
ν_{21}, CH_2 twist + C−H bend + CH_3 bend	1247	**ν_{43}, C−C str + C−O str**	**1249?**	**1242**
		ν_{42}, C−C str + C−O str + C−N str	1251	
ν_{20}, C−C str + CH_2 twist	1264	ν_{41}, C−C str + C−O str + C−N str	1261	
ν_{19}, C−C str	1301	**ν_{40}, C−C str + C−O str + C−N str**	**1261**	**1294**
		ν_{39}, CH_2 wag + CH_3 bend	1334	
ν_{18}, CH_2 wag + CH_3 bend	1335	ν_{38}, CH_2 wag + CH_3 bend	1335	
		ν_{37}, C−C str + CH_2 wag	1358	
ν_{17}, C−C str + C−O str + CH_2 wag	1364	ν_{36}, C−C str + CH_2 wag	1360	
		ν_{35}, C−C str + CH_2 wag	1370	
ν_{16}, C−C str + C−N str + C−O str	1376	**ν_{34}, C−C str + N=N str**	**1374**	**1375**
		ν_{33}, C−C str + N=N str	**1407**	**1407**
		ν_{32}, CH_3 bend	1416	
ν_{15}, CH_3 bend	1415	ν_{31}, CH_3 bend	1416	
		ν_{30}, C−C str + C−H sciss	1426	
ν_{14}, CH_2 sciss + CH_3 bend	1433	ν_{29}, CH_2 sciss + CH_3 bend	1435	
		ν_{28}, C−C str + CH_2 sciss	1436	
		ν_{27}, C−C str + C−O str + CH_2 sciss	1446	
		ν_{26}, CH_2 sciss + CH_3 bend	1450	
ν_{13}, CH_2 sciss + CH_3 bend	1451	**ν_{25}, C−C str + N=N str**	**1453**	**1452**
		ν_{24}, C−C str + C−N str	**1484?**	
ν_{12}, C−C str	1527	**ν_{23}, C−C str + C−N str + N=N str**	**1486?**	**1485**
		ν_{22}, C−C str + C−O str	1568	
ν_{11}, C−C str	1572	ν_{21}, C−C str + N=N str	1572	
		ν_{20}, C−C str	1612	
		ν_{19}, C−C str + C−O str + N=N str	**1616**	**1600**
ν_{10}, N=C=C asymm str	1886			

[a] Experimental vibrational frequencies are compared to those from UBPW91/cc-PVDZ computations for the singlet and triplet states of 4-ethoxyphenyl nitrene (A) and those from Bpw91/cc-Pvdz computations for the potential 4-ethoxyphenyl nitrene dehydroazepine and azo products (B). See text for more details. Possible vibrational band assignments are also shown on the basis of comparison to calculated vibrational frequencies from UBPW91/cc-PVDZ or BPW91/cc-PVDZ computations in the 750- to 1700-cm^{-1} fingerprint region for the ground singlet and triplet states of 4-ethoxyphenyl nitrene and the ground singlet state of its dehydroazepine or azo products (see text).

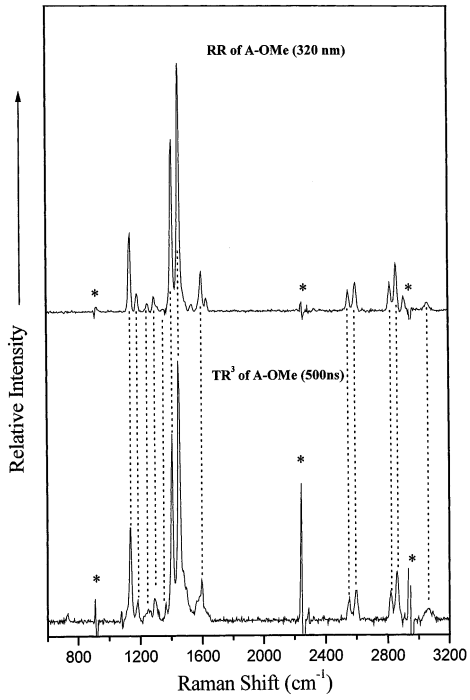

Figure 6. Comparison of the 320-nm resonance Raman spectrum (top) of the authentic 4,4′-dimethoxyazobenzene sample to the TR^3 spectrum (bottom) obtained at 500 ns following 266-nm photolysis of 4-methoxyphenyl azide using a 320-nm probe wavelength. Asterisks mark solvent-subtraction artifacts, and daggers represent small stray-light or ambient-light artifacts.

an intermediate that does not absorb at the 416-nm probe wavelength used in those experiments.[56] This dark intermediate species then decays and produces the ring-expansion dehydroazepine product of 2-fluorenyl nitrene on the 5−10 μs timescale. Since dehydroazepine products are generally associated with formation from singlet arylnitrenes, the 2-fluorenylnitrene species was assigned to the singlet state.[56] A comparison of the time-resolved resonance Raman results for the triplet 4-methoxyphenyl nitrene and 4-ethoxyphenyl nitrene reactions presented here and the previously examined 2-fluorenyl nitrene reaction[56] provide direct spectroscopic experimental evidence that triplet arylnitrenes and singlet arylnitrenes mainly decay via distinctly different kinds of reaction mechanisms insofar as they are representative of arylnitrene reactions. The longer-lived triplet arylnitrene appears to decay mainly via a bimolecular dimerization reaction to directly produce azo dimer products, in agreement with numerous previous investigations.[7,8,15,50] However, the singlet arylnitrene decays via unimolecular processes either to form the triplet arylnitrene via ISC or to form an intermediate species (that does not absorb in the 400−430-nm region) that subsequently produces the dehydroazepine ring-expansion product on the microsecond time scale in the case of the 2-fluorenyl nitrene system. This supports the prediction of Karney and Borden[42] that arylnitrene ring-expansion reactions proceed via a two-step mechanism where the arylnitrene first forms an intermediate species (proposed by Karney and Borden to be an azirine species) that then forms the dehydroazepine product(s). The production of fluorinated azirine intermediates from fluorinated phenyl nitrenes has been observed in low-temperature matrices by infrared and UV/vis absorption spectroscopy.[37] The azirines have a strong absorption at about 250 nm but exhibit little absorption in the 350- to 450-nm region,[37] and this is consistent with the hypothesis that the dark intermediate in the time-resolved 416-nm resonance Raman spectra for the 2-fluorenyl nitrene decay and formation of its dehydroazepine product is an azirine intermediate.[56]

Previous laser flash photolysis experiments indicate that ultraviolet photolysis of 4-methoxyphenyl azide produces both triplet 4-methoxyphenyl nitrene (with a strong absorption at ∼330 nm) and dehydroazepine ring-expansion products (ketenimine species with a strong absorption in the 350- to 430-nm region).[50] These previous experiments by Platz and co-workers[50] also showed that the azo dimer product formed from the triplet arylnitrenes absorbs strongly in the 300- to 400-nm region. We do not observe the dehydroazepine (or ketenimine) ring-expansion product in our present time-resolved resonance Raman experiments using a 320-nm probe wavelength. This indicates that the dehydroazepine (or ketenimine) ring-expansion product does not absorb very strongly at 320 nm compared to the absorption of triplet 4-methoxyphenyl nitrene or its azo dimer product. Recent experiments using a 416-nm probe wavelength readily showed the 2-fluorenyl nitrene species and its dehydroazepine ring-expansion product(s).[56] This and our present results using a 320-nm probe wavelength indicate that arylnitrene reactions to form azo dimer products and dehydroazepine ring-expansion products can be directly and selectively examined by using appropriate probe wavelengths in time-resolved resonance Raman experiments. This may be useful in selectively examining singlet and triplet states of arylnitrenes and their reactions to form azo dimer and dehydroazepine ring-expansion products in a number of systems. This could also be very useful in comparing the relative chemical reactivity of these species toward a variety of substrates. We plan to explore a range of arylnitrenes and their chemical reactions in the future.

Acknowledgment. This work was supported by grants from the Committee on Research and Conference Grants (CRCG), the Research Grants Council (RGC) of Hong Kong (HKU 7112/00P), and the Large Items of Equipment Allocation 1993−94 from the University of Hong Kong. We thank Miss Tracy But and Professor Patrick H. Toy for their generous synthesis and characterization of an authentic sample of 4,4′-dimethoxyazobenzene.

Supporting Information Available: Additional details of the synthesis and characterization of the 4-methoxyphenyl azide and 4-ethoxyphenyl azide precursor compounds and an authentic sample of 4,4′-dimethoxyazobenzene. Selected output from the density functional theory computations for the singlet and triplet states of the 4-methoxyphenyl nitrene and 4-ethoxyphenyl nitrene species as well as their possible azo dimer and dehydroazepine products. This material is available free of charge via the Internet at http://pubs.acs.org.

References and Notes

(1) Scriven, E. F. V. In *Reactive Intermediates*; Abramovich, R. A., Ed.; Plenum Publishing: New York, 1982; Vol. 2, Chapter 1.

(2) Wentrup, C. *Reactive Molecules*; Wiley-Interscience: New York, 1984; Chapter 4.

(3) Platz, M. S. In *Azides and Nitrenes: Reactivity and Utility*; Scriven, E. F. V., Ed.; Academic Press: New York, 1984; Chapter 7.

(4) Platz, M. S.; Maloney, V. M. In *Kinetics and Spectroscopy of Carbenes and Biradicals*; Platz, M. S., Ed.; Plenum Publishing: New York, 1990; pp 303−320.

(5) Platz, M. S.; Leyva, E.; Haider, K. *Org. Photochem.* **1991**, *11*, 367.

(6) Schuster, G. B.; Platz, M. S. *Adv. Photochem.* **1992**, *17*, 69.

(7) Platz, M. S. *Acc. Chem. Res.* **1995**, *28*, 487.

(8) Borden, W. T.; Gritsan, N. P.; Hadad, C. M.; Karney, W. L.; Kemnitz, C. R.; Platz, M. S. *Acc. Chem. Res.* **2000**, *33*, 765.

(9) Schrock, A. K.; Schuster, G. B. *J. Am. Chem. Soc.* **1984**, *106*, 5228.

(10) Donnelly, T.; Dunkin, I. R.; Norwood, D. S. D.; Prentice, A.; Shields, C. J.; Thomson, P. C. P. *J. Chem. Soc., Perkin Trans. 2* **1985**, 307.
(11) Dunkin, I. R.; Donnelly, T.; Lockhart, T. S. *Tetrahedron Lett.* **1985**, *26*, 359.
(12) Leyva, E.; Platz, M. S. *Tetrahedron Lett.* **1985**, *26*, 2147.
(13) Leyva, E.; Platz, M. S.; Persy, G.; Wirz, J. *J. Am. Chem. Soc.* **1986**, *108*, 3783.
(14) Shields, C. J.; Chrisope, D. R.; Schuster, G. B.; Dixon, A. J.; Poliakoff, M.; Turner, J. J. *J. Am. Chem. Soc.* **1987**, *109*, 4723.
(15) Li, Y.-Z.; Kirby, J. P.; George, M. W.; Poliakoff, M.; Schuster, G. B. *J. Am. Chem. Soc.* **1988**, *110*, 8092.
(16) Poe, R.; Grayzar, J.; Young, M. J. T.; Leyva, E.; Schnapp, K.; Platz, M. S. *J. Am. Chem. Soc.* **1991**, *113*, 3209.
(17) Young, M. J. T.; Platz, M. S. *J. Org. Chem.* **1991**, *56*, 6403.
(18) Poe, R.; Schnapp, K.; Young, M. J. T.; Grayzar, J.; Platz, M. S. *J. Am. Chem. Soc.* **1992**, *114*, 5054.
(19) Younger, C. G.; Bell, R. A. *J. Chem. Soc., Chem. Commun.* **1992**, 1359.
(20) Kim, S.-J.; Hamilton, T. P.; Schaefer, H. F. *J. Am. Chem. Soc.* **1992**, *114*, 5349.
(21) Hrovat, D. A.; Waali, E. E.; Borden, W. T. *J. Am. Chem. Soc.* **1992**, *114*, 8698.
(22) Marcinek, A.; Platz, M. S. *J. Phys. Chem.* **1993**, *97*, 12674.
(23) Marcinek, A.; Leyva, E.; Whitt, D.; Platz, M. S. *J. Am. Chem. Soc.* **1993**, *115*, 8609.
(24) Schnapp, K. A.; Poe, R.; Leyva, E.; Soundarajan, N.; Platz, M. S. *Bioconjugate Chem.* **1993**, *4*, 172.
(25) Schnapp, K. A.; Platz, M. S. *Bioconjugate Chem.* **1993**, *4*, 178.
(26) Anderson, G. B.; Falvey, D. E. *J. Am. Chem. Soc.* **1993**, *115*, 9870.
(27) Davidse, P. A.; Kahley, M. J.; McClelland, R. A.; Novak, M. *J. Am. Chem. Soc.* **1994**, *116*, 4513.
(28) Marcinek, A.; Platz, M. S.; Chan, Y. S.; Floresca, R.; Rajagopalan, K.; Golinski, M.; Watt, D. *J. Phys. Chem.* **1994**, *98*, 412.
(29) Lamara, K.; Redhouse, A. D.; Smalley, R. K.; Thompson, J. R. *Tetrahedron* **1994**, *50*, 5515.
(30) McClelland, R. A.; Davidse, P. A.; Haczialic, G. *J. Am. Chem. Soc.* **1995**, *117*, 4173.
(31) Robbins, R. J.; Yang, L. L.-N.; Anderson, G. B.; Falvey, D. E. *J. Am. Chem. Soc.* **1995**, *117*, 6544.
(32) Srivastava, S.; Falvey, D. E. *J. Am. Chem. Soc.* **1995**, *117*, 10186.
(33) McClelland, R. A.; Kahley, M. J.; Davidse, P. A. *J. Phys. Org. Chem.* **1996**, *9*, 355.
(34) McClelland, R. A.; Kahley, M. J.; Davidse, P. A.; Hadzialic, G. *J. Am. Chem. Soc.* **1996**, *118*, 4794.
(35) Robbins, R. J.; Laman, D. M.; Falvey, D. E. *J. Am. Chem. Soc.* **1996**, *118*, 8127.
(36) Moran, R. J.; Falvey, D. E. *J. Am. Chem. Soc.* **1996**, *118*, 8965.
(37) Morawietz, J.; Sander, W. *J. Org. Chem.* **1996**, *61*, 4351.
(38) Castell, O.; Garcia, V. M.; Bo, C.; Caballol, R. *J. Comput. Chem.* **1996**, *17*, 42.
(39) Michalak, J.; Zhai, H. B.; Platz, M. S. *J. Phys. Chem.* **1996**, *100*, 14028.
(40) Karney, W. L.; Borden, W. T. *J. Am. Chem. Soc.* **1997**, *119*, 1378.
(41) Karney, W. L.; Borden, W. T. *J. Am. Chem. Soc.* **1997**, *119*, 3347.
(42) Gritsan, N. P.; Yuzawa, T.; Platz, M. S. *J. Am. Chem. Soc.* **1997**, *119*, 5059.
(43) Born, R.; Burda, C.; Senn, P.; Wirz, J. *J. Am. Chem. Soc.* **1997**, *119*, 5061.
(44) Gritsan, N. P.; Zhai, H. B.; Yuzawa, T.; Karweik, D.; Brooke, J.; Platz, M. S. *J. Phys. Chem. A* **1997**, *101*, 2833.
(45) Moran, R. J.; Falvey, D. E. *J. Am. Chem. Soc.* **1996**, *118*, 8965.
(46) Srivastava, S.; Toscano, J. P.; Moran, R. J.; Falvey, D. E. *J. Am. Chem. Soc.* **1997**, *119*, 11552.
(47) Leyva, E.; Sagredo, R. *Tetrahedron* **1998**, *54*, 7367.
(48) Gritsan, N. P.; Zhu, Z.; Hadad, C. M.; Platz, M. S. *J. Am. Chem. Soc.* **1999**, *121*, 1202.
(49) Gritsan, N. P.; Gudmundsdottir, A. D.; Tigelaar, D.; Platz, M. S. *J. Phys. Chem. A* **1999**, *103*, 3458.
(50) Gritsan, N. P.; Tigelaar, D.; Platz, M. S. *J. Phys. Chem. A* **1999**, *103*, 4465.
(51) Cerro-Lopez, M.; Gritsan, N. P.; Zhu, Z.; Platz, M. S. *J. Phys. Chem. A* **2000**, *104*, 9681.
(52) Srivastava, S.; Ruane, P. H.; Toscano, J. P.; Sullivan, M. B.; Cramer, C. J.; Chiapperino, D.; Reed, E. C.; Falvey, D. E. *J. Am. Chem. Soc.* **2000**, *122*, 8271.
(53) Gritsan, N. P.; Likhotvorik, I.; Tsao, M.-L.; Celebi, N.; Platz, M. S.; Karney, W. L.; Kemnitz, C. R.; Borden, W. T. *J. Am. Chem. Soc.* **2001**, *123*, 1425.
(54) Zhu, P.; Ong, S. Y.; Chan, P. Y.; Leung, K. H.; Phillips, D. L. *J. Am. Chem. Soc.* **2001**, *123*, 2645.
(55) Zhu, P.; Ong, S. Y.; Chan, P. Y.; Poon, Y. F.; Leung, K. H.; Phillips, D. L. *Chem.—Eur. J.* **2001**, *7*, 4928.
(56) Ong, S. Y.; Zhu, P.; Poon, Y. F.; Leung, K.-H.; Fang, W. H. *Chem.—Eur J.* **2002**, *8*, 2163.
(57) (a) Brown, B. R.; Yielding, L. W.; White, W. E., Jr. *Mutat. Res.* **1980**, *70*, 17. (b) White, W. E., Jr.; Yielding, L. W. In *Methods in Enzymology: Affinity Labeling*; Jakoby, W. B., Wilchek, M., Eds.; Academic Press: Orlando, FL, 1977; Vol. 46, pp 646−647.
(58) Wheeler, O. H.; Gonzalez, D. *Tetrahedron* **1964**, *20*, 189.
(59) Li, Y.-L.; Leung, K. H.; Phillips, D. L. *J. Phys. Chem. A* **2001**, *105*, 1061.
(60) Li, Y.-L.; Chen, D.-M.; Wang, D.; Phillips, D. L. *J. Org. Chem.* **2002**, *67*, 4228.
(61) Frisch, M. J.; Trucks, G. W.; Schlegel, H. B.; Scuseria, G. E.; Robb, M. A.; Cheeseman, J. R.; Zakrzewski, V. G.; Montgomery, J. A., Jr.; Stratmann, R. E.; Burant, J. C.; Dapprich, S.; Millam, J. M.; Daniels, A. D.; Kudin, K. N.; Strain, M. C.; Farkas, O.; Tomasi, J.; Barone, V.; Cossi, M.; Cammi, R.; Mennucci, B.; Pomelli, C.; Adamo, C.; Clifford, S.; Ochterski, J.; Petersson, G. A.; Ayala, P. Y.; Cui, Q.; Morokuma, K.; Malick, D. K.; Rabuck, A. D.; Raghavachari, K.; Foresman, J. B.; Cioslowski, J.; Ortiz, J. V.; Stefanov, B. B.; Liu, G.; Liashenko, A.; Piskorz, P.; Komaromi, I.; Gomperts, R.; Martin, R. L.; Fox, D. J.; Keith, T.; Al-Laham, M. A.; Peng, C. Y.; Nanayakkara, A.; Gonzalez, C.; Challacombe, M.; Gill, P. M. W.; Johnson, B. G.; Chen, W.; Wong, M. W.; Andres, J. L.; Head-Gordon, M.; Replogle, E. S.; Pople, J. A. *Gaussian 98*; Gaussian, Inc.: Pittsburgh, PA, 1998.
(62) Becke, A. *J. Chem. Phys.* **1986**, *84*, 4524.
(63) Wang, Y.; Perdew, J. P. *Phys. Rev. B* **1991**, *44*, 13298.
(64) Dunning, T. H. *J. Chem. Phys.* **1989**, *90*, 1007.
(65) Koida, S.; Udagawa, N.; Mikama, N.; Kaya, K.; Ito, M. *Bull. Chem. Soc. Jpn.* **1972**, *45*, 3542.
(66) Houben, J. L.; Masetti, G.; Campani, E.; Gorini, G. *J. Raman Spectrosc.* **1982**, *13*, 15.
(67) Okamoto, H.; Hamaguchi, H.; Tasumi, M. *Chem. Phys. Lett.* **1986**, *130*, 185.
(68) Biancalana, A.; Campani, E.; Gorini, G.; Masetti, G.; Quaglia, M. *J. Raman Spectrosc.* **1992**, *23*, 155.
(69) Biswas, N.; Umapathy, S. *Chem. Phys. Lett.* **1995**, *236*, 24.
(70) Biswas, N.; Umapathy, S. *J. Chem. Phys.* **1997**, *107*, 7849.
(71) Biswas, N.; Umapathy, S. *Chem. Phys. Lett.* **1998**, *294*, 181.
(72) Fujino, T.; Tahara, T. *J. Phys. Chem. A* **2000**, *104*, 4203−4210.